A "Véges rugalmas-képlékeny alakváltozás elméleti és numerikus vizsgálata" című OTKA kutatási téma rövid szakmai összefoglalója

Az OTKA téma keretében végzett kutatásokat az alábbi pontok foglalják össze.

- A mikropoláris testek alakváltozási és feszültségi állapotának számítására egy háromdimenziós végeselemes eljárást dolgoztunk ki, 20 csomópontos izoparaméteres elemek felhasználásával. Az elem csomópontjaiban 3 elmozdulás és három (az elmozdulásmezőtől független) forgás koordináta van értelmezve. A végeselemes programban az Eringen-féle mikropoláris test leíró egyenletei kerültek beépítésre. A lineárisan rugalmas modellt kiterjesztettük a kis rugalmas-képlékeny alakváltozási tartományba. A mikropoláris testre vonatkozó rugalmas torzítási energia alapján módosítottuk a Mises-féle képlékenységi feltételt. Az egyenértékű feszültség számítására vonatkozó összefüggés a feszültség tenzor mellett a feszültségpár tenzort is tartalmazza. Ezt röviden az alábbi egyenletek foglalják össze (*Gombos, Szabó [2,4,3-w]*): a *módosított Mises-féle képlékenységi feltétel*:

$$F(\mathbf{t}, \mathbf{m}, R(\alpha)) = \sqrt{2J_2} - R(\alpha) \leq 0$$

ahol

$$J_2 = \frac{1}{2}\left(\mathbf{s}_S : \mathbf{s}_S + \frac{1-\mathcal{N}^2}{\mathcal{N}^2}\mathbf{s}_A : \mathbf{s}_A + \frac{1}{l_t^2}\mathbf{m}_{dS} : \mathbf{m}_{dS} + \frac{1}{4l_b^2 - l_t^2}\mathbf{m}_{dA} : \mathbf{m}_{dA}\right).$$

Itt $\mathbf{s}_S$, $\mathbf{s}_A, \mathbf{m}_{dS}$ és $\mathbf{m}_{dA}$ a deviátoros feszültségi és feszültségpár tenzor szimmetrikus és ferdén szimmetrikus része, $\mathcal{N}, l_t$ és l_b mikropoláris anyagparaméterek, $R(\alpha)$ keményedési függvény.

- A rugalmas-képlékeny konstitutív egyenlet integrálására rugalmas-ideálisan képlékeny anyagmodell esetén analitikus megoldást állítottunk elő. Keményedő esetben a programba a "Return mapping" eljárást építettük be. Mindkét eljáráshoz kidolgoztuk a konzisztens érintő mátrixot(*Gombos,Szabó[2,4,2-w,3-w,5-w]*).

- Kétdimenziós rugalmasságtani feldatok megoldására a meshless eljáráson alapuló programot dolgoztunk ki. A programot kiterjesztettük a peridynamikus modell számítására is(*Ladányi [5,6,7]*).

- Egy kristályok véges alakváltozásának számítására különböző algoritmusokat dolgoztunk ki. A teljes konstitutív egyenletrendszerben a rugalmas alakváltozást leíró modelleket külön vizsgáltuk különböző hiper és hipoelasztikus anyagmodellek alapján. Egy és két csúszási rendszert tartalmazó nyírási feladaton összehasonlító számítások történtek. Az eredmények alapján jól körülhatárolható az az alakváltozási tartomány, ahol már jelentőséggel bírnak a rugalmas modellek.(*Kossa,Szabó[1,3]*)

- A klasszikus Prandtl-Reuss elmélet konstitutív egyenletének integrálására analitikus eljárást dolgoztunk ki lineárisan izotrop keményedési modell esetén. A megoldás az "incomplete Beta" függvények alkalmazásán alapul(*Szabó[1-w]*).

- Az izotrop modellre kidolgozott eljárást továbbfejlesztettük a kombinált izotrop-kinematikai modellre. Mivel számos végeselemes program az egytengelyű feszültség-képlékeny alakváltozás görbét lineáris szegmensekből építi fel, ezért a javasolt egzakt integrálási eljárás a gyakorlati alkalmazás szemponjából nagy jelentőséggel bír (*Kossa, Szabó [4-w,6-w]*).

Publikációk

Konferencia előadások, konferencia kiadványokban megjelent összefoglalók

[1] Kossa, A., Szabó L., Using logarithmic stress rate in computational single crystal plasticity, 35th SOLID MECHANICS CONFERENCE, Kraków, Poland, September 4-8, 2006.

[2] Gombos Á., Szabó L., Computational aspects of micropolar elastoplasticity, 35th SOLID MECHANICS CONFERENCE, Kraków, Poland, September 4-8, 2006.

[3] Kossa A., Szabó L., Logarithmic stress rate in single crystal plasticity, 6th European Solid Mechanics Conference (ESMC 2006), 28 August - 1 September 2006, Budapest, Hungary

[4] Gombos Á., Szabó L., Computational aspects of micropolar elastoplasticty, 6th European Solid Mechanics Conference (ESMC 2006), 28 August - 1 September 2006, Budapest, Hungary

[5] Ladányi G., Application of MESHLESS method on field of elasticity, MicroCAD 2004, Miskolc.

[6] Ladányi G., Numerical analysis of peridynamic material with moving least square method, ECCOMAS Thematic Conference on Meshless Methods, 2005.Liszabon, Portugália.

[7] Ladányi G., Analisys of Peridynamic Material model with RBF method, 6th European Solid Mechanics Conference (ESMC 2006), 28 August - 1 September 2006, Budapest, Hungary

Kidolgozás alatt álló folyóírat cikkek, konferencia előadások

[1-w] Szabó L., A semi-analitical integration method for J2 flow theory of plasticity with linear isotropic hardening, (in preparation, 80%) *Computer. Methods. Appl. Mech. Engrg.*

[2-w] Szabó L., Gombos Á., Exact stress update of non-hardening micropolar elastoplasticity at small deformation, (in preparation,80%) *Computers & Structures*

[3-w] Gombos Á, Szabó L., Computational aspects of micropolar elastoplasticity, (in preparation, 60%) *Computers & Structures*

[4-w] Kossa, A., Szabó L., A new integration method for von Mises plasticity model with linear isotropic and kinematic hardening, (in preparation, 20%) *Int. J. of Plasticity*

[5-w] Gombos Á, Szabó L., Mikropoláris testek rugalmas-képlékeny alakváltozásának végeselemes számítási eljárásai, MaMeK, 2007. augusztus 27-29.

[6-w] Kossa, A., Szabó L., Véges rugalmas-képlékeny alakváltozás végeselemes számítási módszerei, MaMeK, 2007. augusztus 27-29.

POLISH ACADEMY OF SCIENCES

INSTITUTE OF FUNDAMENTAL TECHNOLOGICAL RESEARCH

35th Solid Mechanics Conference

Kraków, September 4 - 8, 2006

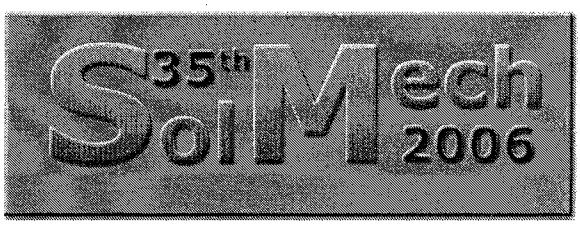

VOLUME OF ABSTRACTS

COMPUTATIONAL ASPECTS OF MICROPOLAR ELASTOPLASTICITY

Á. Gombos, L. Szabó
Department of Applied Mechanics, Budapest University of Technology and Economics, Budapest, Hungary

1. Introduction

The micropolar continuum model have been fairly extensively analysed in the last decad. The Cosserat theory have been employed to the J_2-flow theory by de Borst [2], Willam at el. [6], and to the deformation theory by Mülhaus and Vardoulakis [5] in two dimensional range at small deformation. A more general elastoplastic micropolar models in the large deformation range developed by Forest [3] and Grammenoudis and Tsakmakis [4]. However, despite considerable theoretical and computational contributions made in the computational analysis of micropolar continua, many questions are still unanswered and useful formulations similar to the classical continuum plasticity are not available in the literature.

The purpose of this paper is to develop a stress updating algorithm to elastoplastic micropolar solid, and to derive the corresponding consistent (algorithmic) tangent operator to three dimensional case at small deformation. The elastic part of the constitutive model is based on the Eringen's [1] micropolar theory, and the plastic part is defined by an extended Mises-type flow theory of plasticity. The yield function considered in this work is obtained by a consistent derivation of distortion strain energy, so it represents by the deviatoric parts of the stress and the couple stress. In addition, in the case of perfect plasticity an analytical solution of time integration of the constitutive equation is presented.

2. Constitutive relations for micropolar solids

The kinematic equations for micropolar continuum at small deformation are of the form (Eringen [1]): $\varepsilon = \mathrm{grad}^T \mathbf{u} + (\epsilon \cdot \boldsymbol{\phi})^T$, $\boldsymbol{\gamma} = \mathrm{grad}\,\boldsymbol{\phi}$, where $\mathbf{u}$ is the displacement vector, $\boldsymbol{\phi}$ is the microrotation vector, ε and $\boldsymbol{\gamma}$ are the strain measures.

The rate form of the elastic-plastic constitutive equations in the case of small deformation can be summarized as

$$(1)\quad \dot{\mathbf{t}} = \mathbf{A}^e : (\dot{\varepsilon} - \dot{\varepsilon}^p), \qquad \dot{\mathbf{m}}^T = \mathbf{B}^e : (\dot{\boldsymbol{\gamma}} - \dot{\boldsymbol{\gamma}}^p), \qquad \dot{\varepsilon}^p = \lambda \frac{\partial f}{\partial \mathbf{t}}, \quad \dot{\boldsymbol{\gamma}}^p = \lambda \frac{\partial f}{\partial \mathbf{m}^T}, \quad \dot{\alpha} = \lambda h(\mathbf{t}, \mathbf{m});$$

where $\mathbf{t}$ is the stress, $\mathbf{m}$ is the couple stress tensor, λ is the plastic multiplier, α is a hardening parameter, and $\mathbf{A}^e$ and $\mathbf{B}^e$ are the fourth-order elastic constitutive moduli.

The extended form of the von Mises yield condition takes the form

$$(2)\qquad F(\mathbf{t}, \mathbf{m}, \kappa(\alpha)) = \sqrt{2 J_2(\mathbf{t}, \mathbf{m})} - \sqrt{\frac{2}{3}} \kappa(\alpha) \leq 0,$$

where the function $\kappa(\alpha)$ defines the hardening law, and $J_2(\mathbf{t}, \mathbf{m})$ defined as

$$(3)\qquad J_2(\mathbf{t}, \mathbf{m}) = \frac{1}{2} \left(\mathbf{s}_S : \mathbf{s}_S + \frac{(2\mu + \kappa)}{\kappa} \mathbf{s}_A : \mathbf{s}_A + \frac{2\mu + \kappa}{\beta + \gamma} \mathbf{m}_{dS} : \mathbf{m}_{dS} - \frac{2\mu + \kappa}{\beta - \gamma} \mathbf{m}_{dA} : \mathbf{m}_{dA} \right).$$

Here μ, κ, β and γ are the micropolar material parameters, and $\mathbf{s}_S, \mathbf{s}_A$, $\mathbf{m}_{dS}$ and $\mathbf{m}_{dA}$ are the symmetric and skew-symmetric parts of the stress and couple stress, respectively.

3. Stress updating algorithm and consistent tangent operator

In this work, the implicit backward Euler method is employed to determine the updated stress and plastic state variables. In the strain driven problem, the Newton-Raphson iteration privides the strains $\boldsymbol{\varepsilon}_{n+1}$ and $\boldsymbol{\gamma}_{n+1}$ values which use to define the stress and couple stress at step $n+1$ as

$$\mathbf{t}_{n+1} = \mathbf{t}_{n+1}^{trial} - \Delta\lambda \mathbf{A}^e : \left.\frac{\partial f}{\partial \mathbf{t}}\right|_{n+1} \qquad \mathbf{m}_{n+1}^T = \left(\mathbf{m}_{n+1}^{trial}\right)^T - \Delta\lambda \mathbf{B}^e : \left.\frac{\partial f}{\partial \mathbf{m}^T}\right|_{n+1}, \tag{4}$$

where $\mathbf{t}_{n+1}^{trial}$ and $\mathbf{m}_{n+1}^{trial}$ are the so-called trial stress and couple stress, respectively. The set of equations (4) with the yield condition $F_{n+1}(\mathbf{t}_{n+1}, \mathbf{m}_{n+1}, \kappa(\alpha_{n+1})) = 0$ a set of nonlinear equation in terms of values $\mathbf{t}_{n+1}$, $\mathbf{m}_{n+1}$ and $\Delta\lambda$ which is effectively solved by a local Newton iterative procedures.

The consistent tangent operator is essential to preserve the quadratic rate of asymptotic convergence of global Newton-Raphson iteration. To derive this quantity, we use the standard method, and by linearizing the algorithm considered above we obtained the formulas

$$d\mathbf{t} = \mathbf{A}_c^{ep} : d\Delta\boldsymbol{\varepsilon} - \mathbf{C}_c^{ep} : d\Delta\boldsymbol{\gamma}, \quad d\mathbf{m}^T = \mathbf{B}_c^{ep} : d\Delta\boldsymbol{\gamma} - \mathbf{C}_c^{epT} : d\Delta\boldsymbol{\varepsilon}, \tag{5}$$

where the consistent tangent moduli, $\mathbf{A}_c^{ep}$, $\mathbf{B}_c^{ep}$ and $\mathbf{C}_c^{ep}$ are expressed in explicit form.

The algorithm and the consistent tangent operator has been implemented in a finite element code based on 20-noded solid element type. Some numerical examples are presented that demonstrate the capability and accuracy of the proposed algorithm.

In the case of non-hardening micropolar plasticity a closed-form solution is given to the time integration of the constitutive equations with constant strain rate assumption. This analytical solution will serves as a reference for the numerical solutions. The errors in stress and couple stress predictions are analysed for the radial return and the tangent predictor-radial return methods.

Acknowledgment

This research has been supported by the National Development and Research Foundation, Hungary (under Contract: OTKA, T046488). This support is gratefully acknowledged.

References

[1] A.C. Eringen (1999). Microcontinuum Field Theories, Springer Verlag, Berlin.

[2] R. De Borst (1993). A generalisation of J_2-flow theory for polar continua. Comp. Meth. Appl. Mech. Engng, **103**, 347-362.

[3] S. Forest and R. Sievert (2003). Elastoviscoplasticity constitutive frameworks for generalized continua. Acta Mechanica, **160**, 71-111.

[4] P. Grammenoudis and Ch. Tsakmakis (2005). Finite element implementation of large deformation micropolar plasticity exhibiting isotropic and kinematic hardening effects. Int. J. Num. Meth. Engng., **62**, 1691-1720.

[5] H.-B. Mülhaus and I. Vardoulakis (1987). The thickness of shear bands in granular materials. Géotechnique, **37**, 271-283.

[6] K. Willam, A. Dietsche, M-M. Iordache and P. Steinmann (1995). Localization in Micropolar Continua, In: H.-B. Mühlhaus (Ed.), Continuum Models for Materials with Microstructure. John Wiley & Sons, Chichester, 1-25.

USING LOGARITHMIC STRESS RATE IN COMPUTATIONAL SINGLE CRYSTAL ELASTOPLASTICITY

A. Kossa, L. Szabó
Department of Applied Mechanics, Budapest University of Technology and Economics
H-1111 Budapest, Műegyetem rkp. 5., Hungary

1. Introduction

In crystal plasticity at finite strain the constitutive relations usually is expressed in terms of the relation between an objective stress rate and the rate of deformation. In most cases the elastic part of the constitutive equation is a spatial hypoelastic rate equation [1],[4],[5].

This paper presents a constitutive model of single crystal elastoplasticity. The hypoelastic relation implemented in this model based on the logarithmic stress rate, and its integrated form associated with Hencky's hyperelastic relation [6],[7]. In addition, a numerical algorithms for the proposed model is also presented. Some numerical results illustrate the capability and performance of the present model in modelling large elastoplastic deformation of single crystal.

2. Kinematics of single crystals at finite deformation

In crystal plasticity the total deformation gradient $\mathbf{F}$ can be written in the form $\mathbf{F}=\mathbf{F}^{*}\mathbf{F}^{p}$, where $\mathbf{F}^{p}$ is the plastic deformation solely due to plastic shearing on crystallographic slip systems and $\mathbf{F}^{*}$ is a non-plastic deformation gradient which contain the stretching and rotation of the crystal lattice. In the reference configuration $\mathbf{s}_{\alpha}^{0}$ and $\mathbf{m}_{\alpha}^{0}$ are an unit vector along a slip direction and an unit normal of a slip plane, respectively, of the α-th slip system. The Eulerian velocity gradient may be decomposed into a part due to slip-induced plastic deformation, and a part due to elastic deformation, as follows:

$$\mathbf{l}=\dot{\mathbf{F}}\mathbf{F}^{-1}=\dot{\mathbf{F}}^{*}\mathbf{F}^{-1}+\mathbf{F}^{*}\dot{\mathbf{F}}^{p}\mathbf{F}^{p-1}\mathbf{F}^{*-1}=\mathbf{l}^{*}+\dot{\mathbf{F}}^{*}\mathbf{l}^{p}\mathbf{F}^{*-1} \tag{1}$$

Because of the plastic deformation leaves the lattice structure unaffected, therefore $\mathbf{s}_{\alpha}^{0}$ and $\mathbf{m}_{\alpha}^{0}$ are transformed by only the elastic part of the deformation gradient: $\mathbf{s}_{\alpha}=\mathbf{F}^{*}\mathbf{s}_{\alpha}^{0}$ and $\mathbf{m}_{\alpha}=\left(\mathbf{F}^{*}\right)^{-T}\mathbf{m}_{\alpha}^{0}$. In view of this fact, the plastic part of velocity gradient due to crystallographic slip may be expressed by

$$\mathbf{l}^{p}=\dot{\mathbf{F}}^{p}\mathbf{F}^{p-1}=\sum_{\alpha=1}^{n}\dot{\gamma}^{\alpha}\mathbf{s}_{\alpha}^{0}\otimes\mathbf{m}_{\alpha}^{0}=\sum_{\alpha=1}^{n}\dot{\gamma}^{\alpha}\mathbf{Z}_{\alpha}^{0}. \tag{2}$$

The plastic velocity gradient can be resolved uniquely into two parts. The symmetric part $\mathbf{d}^{p}$ is the plastic part of the rate of deformation, and the skew-symmetric part $\mathbf{w}^{p}$ is the plastic part of vorticity:

$$\mathbf{d}^{p}=\sum_{\alpha=1}^{n}\dot{\gamma}^{\alpha}\mathbf{N}_{\alpha}\text{, and }\mathbf{w}^{p}=\sum_{\alpha=1}^{n}\dot{\gamma}^{\alpha}\mathbf{Y}_{\alpha}\text{, where }\mathbf{N}_{\alpha}=\tfrac{1}{2}\left(\mathbf{Z}_{\alpha}+\mathbf{Z}_{\alpha}^{T}\right),\ \mathbf{Y}_{\alpha}=\tfrac{1}{2}\left(\mathbf{Z}_{\alpha}-\mathbf{Z}_{\alpha}^{T}\right). \tag{3}$$

The yield function for the α-th slip system is defined of the form

$$\phi_{\alpha}\left(\tau_{\alpha}\right)=\tau_{\alpha}-\tau_{Y}, \tag{4}$$

where τ_α is the Schmid resolved stress in the α-th slip system:

(5) $$\tau_\alpha = \mathbf{s}_\alpha \boldsymbol{\tau} \mathbf{m}_\alpha = \boldsymbol{\tau} : \mathbf{Z}_\alpha .$$

τ_Y is the resolved yield stress, which is a given function of the accumulated slip $\Gamma = \int_0^t \sum_{\alpha=1}^{n} \dot{\gamma}^\alpha dt$.

Using logarithmic stress-rate in the elastic part of the deformation, we obtain the following hyperelastic constitutive relation [6],[7]:

(6) $$\overset{\circ}{\boldsymbol{\tau}}{}^{*\log} = \mathcal{D}^e : \mathbf{d}^* \quad \Rightarrow \quad \boldsymbol{\tau} = \mathcal{D}^e : \mathbf{h}^*,$$

where $\mathcal{D}^e$ is the fourth rank tensor of elastic moduli, and $\mathbf{h}^* = \ln \mathbf{b}^* = \ln\left(\mathbf{F}^* \mathbf{F}^{*T}\right)$ is the spatial logarithmic strain (*Hencky*-strain), calculated from the elastic part of the deformation gradient.

3. Numerical method

The numerical framework in rate-independent context is based on the implicit approximation to the inelastic flow equation. The differential equation (2) can be numerically integrated in an implicit fashion with use of the tensor exponential [2],[3]:

(7) $$\mathbf{F}^p_{n+1} = \exp\left(\sum_{\alpha=1}^{n} \Delta\gamma^\alpha \mathbf{Z}^0_\alpha\right) \mathbf{F}^p_n, \quad \Rightarrow \quad \mathbf{F}^*_{n+1} = \mathbf{F}_{n+1} \mathbf{F}^{p-1}_n \exp\left(-\sum_{\alpha=1}^{n} \Delta\gamma^\alpha \mathbf{Z}^0_\alpha\right),$$

where $\Delta\gamma^\alpha$ is the plastic slip increment in the time interval $[t_n, t_{n+1}]$. The accumulated slip variable is update by the formula: $\Gamma_{n+1} = \Gamma_n + \sum_{\alpha=1}^{n} \Delta\gamma^\alpha$. The incremental plastic slip must satisfy the incremental plastic consistency criterion:

(8) $$\phi^\alpha\left(\tau_{\alpha,n+1}, \tau_Y\left(\Gamma_{n+1}\right)\right) \le 0, \qquad \Delta\gamma^\alpha \ge 0, \qquad \phi^\alpha\left(\tau_{\alpha,n+1}, \tau_Y\left(\Gamma_{n+1}\right)\right) \Delta\gamma^\alpha \ge 0$$

for all α. The stress update procedure requires the solution of the above non-linear system. Illustrative examples will be presented to demonstrate the performance of the proposed formulation.

Acknowledgment

This research has been supported by the National Development and Research Foundation, Hungary (under Contract: OTKA, T046488). This support is gratefully acknowledged.

References

[1] R.J. Asaro (1999). Micromechanics of crystals and polycrystals, *Advances in Applied Mechanics*, **23**, 1-113.

[2] C. Miehe (1996). Exponential map algorithm for stress updates in anisotropic multiplicative elastoplasticity for single crystals, *International Journal for Numerical Methods in Engineering*, **39**, 3367-3390.

[3] C. Miehe (1996). Multisurface thermoplasticity for single crystals at large strains in terms of eulerian vector updates, *International Journal of Solids and Structures*, **33**, 20-22.

[4] S. Nemat-Nasser (2005). *Plasticity,* Cambridge University Press, Cambridge.

[5] D. Peirce, R.J. Asaro, A. Needleman (1982). An analysis of nonuniform and localized deformation in ductile single crystals, *Acta Metallurgica*, **30**, 1087-1119.

[6] H. Xiao, O.T. Bruhns, A.T.M. Meyers (1998). On Objective Corotational Rates and Their Defining Spin Tensors, *International Journal of Solids and Structures*, **35**, 4001-4014.

[7] H. Xiao, O.T. Bruhns, A.T.M. Meyers (1998). Strain Rates and Material Spins, *Journal of Elasticity*, **52**, 1-41.

6th European Solid Mechanics Conference
ESMC 2006
28 August – 1 September, 2006
Budapest, Hungary

LOGARITHMIC STRESS RATE IN SINGLE CRYSTAL ELASTOPLASTICITY

Attila Kossa[1], and László Szabó[1]

[1]Department of Applied Mechanics
Budapest University of Technology and Economics
H-1111 Budapest, Műegyetem rkp. 5., Hungary
E-mail: kossa@mm.bme.hu ; szabo@mm.bme.hu

Keywords: Crystal plasticity, objective corotational stress rate, logarithmic stress rate.

Summary. *The goal of this paper is to present a constitutive relations in single crytal plasticity using logarithmic stress-rate. This equation is composed of fourth-order elastic-plastic tangent tensor, and the rate of deformation tensor and objective corotational rate of Kirchhoff stress tensor. In addition elastic-plastic relations are derived for other objective corotational stress-rates. A comparative numerical study of derived models is presented by using symbolic mathematical software MAPLE, and finite element program ABAQUS.*

1 INTRODUCTION

In crystal plasticity at finite strain the constitutive equation usually is expressed in terms of the relation between a corotational stress rate and the rate of deformation. In most cases the elastic part of the constitutive equation is a spatial hypoelastic rate equation. In past years, studies demonstrated that in all spatial hypoelastic rate equations only the one based on the logarithmic stress rate is consistent with elasticity [3]. This favorable property can be use in elastic constitutive relation of single crystal plasticity. This paper presents a general elastic-plastic consitutive equation for various corotational stress rates, including logarithmic stress rate. Finally numerical comparisons are presented, using ABAQUS UMAT subroutine and MAPLE symbolic mathematical software.

2 CONSTITUTIVE RELATIONS IN SINGLE CRYSTAL ELASTOPLASTICITY

In crystal plasticity the total deformation gradient $\mathbf{F}$, can be divided into a non-plastic deformation gradient $\mathbf{F}^*$, and a plastic deformation gradient $\mathbf{F}^p$, as follows: $\mathbf{F}=\mathbf{F}^*\mathbf{F}^p$. The velocity gradient $\mathbf{L}$ in the current configuration can be calculated by the following equation: $\mathbf{L}=\dot{\mathbf{F}}\mathbf{F}^{-1}=\mathbf{L}^*+\mathbf{L}^p=\mathbf{d}^*+\mathbf{w}^*+\mathbf{d}^p+\mathbf{w}^p$, where $\mathbf{d}^p$ and $\mathbf{w}^p$ are plastic deformation rate and plastic vorticity, respectively, due to dislocation slip, and $\mathbf{d}^*$ and $\mathbf{w}^*$ are the non-plastic deformation rate and non-plastic spin due to the crystal lattice deformation and rotation. The vector $\mathbf{s}_\alpha$ in the slip direction of the α th slip system at the current state is defined in the following way: $\mathbf{s}_\alpha=\mathbf{F}^*\mathbf{s}_\alpha^0$. To keep vector $\mathbf{m}_\alpha$ normal to the slip plane, the following relation has to be introduced: $\mathbf{m}_\alpha=\mathbf{m}_\alpha^0\mathbf{F}^{*-1}$. The time-rate-of-change of the vectors $\mathbf{s}_\alpha$ and $\mathbf{m}_\alpha$ which define the current direction of the α th slip on the slip plane of normal $\mathbf{m}_\alpha$ are defined by $\dot{\mathbf{s}}_\alpha=\mathbf{L}^*\mathbf{s}_\alpha$, and $\dot{\mathbf{m}}_\alpha=-\mathbf{L}^{*T}\mathbf{m}_\alpha$, respectively. The plastic parts of the rate of deformation and vorticity become

$$\mathbf{d}^p=\dot{\gamma}^\alpha\mathbf{N}_\alpha,\ \text{and}\ \mathbf{w}^p=\dot{\gamma}^\alpha\mathbf{Y}_\alpha, \tag{2.1}$$

where $\mathbf{N}_\alpha=\frac{1}{2}\left(\mathbf{s}_\alpha\otimes\mathbf{m}_\alpha+\mathbf{m}_\alpha\otimes\mathbf{s}_\alpha\right)$, and $\mathbf{Y}_\alpha=\frac{1}{2}\left(\mathbf{s}_\alpha\otimes\mathbf{m}_\alpha-\mathbf{m}_\alpha\otimes\mathbf{s}_\alpha\right)$.

2.1 Elastic constitutive relations

The elastic constitutive relations by using objective corotational stress-rate is defined by:

$$\overset{\circ}{\boldsymbol{\tau}}{}^*=\mathscr{D}^e:\mathbf{d}^*, \tag{2.2}$$

where $\overset{\circ}{\boldsymbol{\tau}}{}^*=\dot{\boldsymbol{\tau}}-\boldsymbol{\Omega}^*\boldsymbol{\tau}+\boldsymbol{\tau}\boldsymbol{\Omega}^*$ is the elastic part of the objective corotational rate of Kirchhoff stress $\boldsymbol{\tau}$, and $\boldsymbol{\Omega}^*$ is the elastic spin tensor, which can be written:

$$\mathbf{\Omega}^* = \mathbf{w}^* + \mathscr{A}^* : \mathbf{d}^*, \tag{2.3}$$

where the expression of the fourth-order tensor $\mathscr{A}^* = \mathscr{A}^*\left(\mathbf{F}^*\mathbf{F}^{*T}\right)$ is different for each objective corotational rate (for example in case of Jaumann-rate tensor $\mathscr{A}^*$ identical to zero).

The elastic constitutive equation, using the relations between total and elastic parts of deformation can be written as:

$$\overset{\circ}{\boldsymbol{\tau}} = \tilde{\mathscr{D}}^e : \left(\mathbf{d} - \dot{\gamma}^\alpha \mathbf{\Theta}_\alpha\right), \tag{2.4}$$

where $\tilde{\mathscr{D}}^e = \mathscr{D}^e + \tilde{\mathscr{M}}$, $\mathbf{\Theta}_\alpha = \left(\mathscr{D}^e + \tilde{\mathscr{M}}\right)^{-1} : \left[\mathscr{D}^e : \mathbf{N}_\alpha - \boldsymbol{\tau}\left(\mathbf{Y}_\alpha + \mathscr{A}^* : \mathbf{N}_\alpha\right) + \left(\mathbf{Y}_\alpha + \mathscr{A}^* : \mathbf{N}_\alpha\right)\boldsymbol{\tau}\right]$. Here $\tilde{\mathscr{M}}$ is defined by:

$$\boldsymbol{\tau}\left[\left(\mathscr{A} - \mathscr{A}^*\right) : \mathbf{d}\right] - \left[\left(\mathscr{A} - \mathscr{A}^*\right) : \mathbf{d}\right]\boldsymbol{\tau} = \tilde{\mathscr{M}} : \mathbf{d}, \quad \tilde{\mathscr{M}}_{ijkl} = \tau_{im}\left(\mathscr{A}_{mjkl} - \mathscr{A}^*_{mjkl}\right) - \left(\mathscr{A}_{mjkl} - \mathscr{A}^*_{mjkl}\right)\tau_{mj}. \tag{2.5}$$

2.2 Elastic-plastic constitutive relations

The hardening law without non-Schmid effect is defined as $\dot{\tau}^{cr}_\alpha = \mathrm{h}_{\alpha\beta}\dot{\gamma}^\beta$, where $\mathrm{h}_{\alpha\beta}$ is the hardening matrix, and τ^{cr}_α is the critical shear strength. Using this hardening law, the equation (2.4) can be reformulated to the widely used form of the elastic-plastic constitutive relation. A straightforward manipulation yields

$$\overset{\circ}{\boldsymbol{\tau}} = \mathscr{D}^{ep} : \mathbf{d}, \tag{2.6}$$

where the fourth-order elastic-plastic tangent tensor $\mathscr{D}^{ep}$ is defined as:

$$\mathscr{D}^{ep} = \left[\mathscr{I} + \tilde{\mathrm{G}}^{\beta\alpha}\left(\tilde{\mathscr{D}}^e : \mathbf{\Theta}_\beta\right) \otimes \mathbf{N}_\alpha\right]^{-1} : \left[\tilde{\mathscr{D}}^e - \tilde{\mathrm{G}}^{\beta\alpha}\left(\tilde{\mathscr{D}}^e : \mathbf{\Theta}_\beta\right) \otimes \left(\mathbf{N}_\alpha : \mathscr{M}\right)\right], \tag{2.7}$$

where $\tilde{\mathrm{G}}^{\beta\alpha} = \left(\tilde{\mathrm{g}}_{\alpha\beta}\right)^{-1}$, and $\tilde{\mathrm{g}}_{\alpha\beta} = \mathrm{h}_{\alpha\beta} + \mathbf{N}_\alpha : \left[\left(\mathbf{N}_\beta - \mathbf{Y}_\beta\right)\boldsymbol{\tau} - \boldsymbol{\tau}\left(\mathbf{N}_\beta - \mathbf{Y}_\beta\right)\right]$, and $\mathscr{I}$ is the the fourth-order unit tensor, and $\tilde{\mathscr{M}}$ is defined by:

$$\left(\mathscr{A} : \mathbf{d}\right)\boldsymbol{\tau} - \boldsymbol{\tau}\left(\mathscr{A} : \mathbf{d}\right) = \mathscr{M} : \mathbf{d}, \quad \mathscr{M}_{ijkl} = \tau_{im}\mathscr{A}_{mjkl} - \mathscr{A}_{imkl}\tau_{mj}, \tag{2.8}$$

where the fourth-order tensor $\mathscr{A} = \mathscr{A}\left(\mathbf{F}\mathbf{F}^T\right)$ is derived from the expression of spin tensor $\mathbf{\Omega}$ respect to the total deformation in the following way:

$$\mathbf{\Omega} = \mathbf{w} + \mathscr{A} : \mathbf{d}. \tag{2.9}$$

3 APPLICATIONS

The consitutive models presented above has been implemented in the finite element program ABAQUS through subroutine UMAT. In possession of material parameters, numerical tests can be perform, using different corotational rates, and the results can be compared. From this comparison, features of corotational rates will appear, which is useful in deciding on an appropriate elastic constitutive relation in single crystal plasticity at large deformation.

ACKNOWLEDGMENT

This research has been supported by the National Development and Research Foundation, Hungary (under Contract: OTKA, T046488). This support is gratefully acknowledged..

REFERENCES

[1] Asaro, R. J. (1999): Micromechanics of crystals and polycrystals, *Advances in Applied Mechanics*, Vol. 23, pp. 1-113.
[2] Bassani, J. L. (1994): Plastic Flow of Crystals, *Advances in Applied Mechanics*, Vol. 30, pp. 191-258.
[3] Lin, R. C. (2002): Analytical stress solutions of a closed deformation path with stretching and shearing using the hypoelastic formulations, *European J. of Mechanics A*, Vol. 22, pp. 443-461.
[4] Nemat-Nasser, S. (2005): *Plasticity,* Cambridge University Press, Cambridge.
[5] Szabó, L., Yatomi, C. (1997): Loss of Strong Ellipticity Condition in Single Crystal Plasticity, *Proceedings of IMMM '97*, pp. 201-208, Mie University Press, Japan.
[6] Xiao, H., Bruhns, O. T. and Meyers, A. T. M. (1998): On Objective Corotational Rates and Their Defining Spin Tensors, *Int. J. Solids Structures*, Vol. 35, pp. 4001-4014.
[7] Xiao, H., Bruhns, O. T. and Meyers, A. T. M. (1998): Strain Rates and Material Spins, *Journal of Elasticity*, Vol. 52, pp. 1-41.

6th European Solid Mechanics Conference
ESMC 2006
28 August – 1 September, 2006
Budapest, Hungary

COMPUTATIONAL ASPECTS OF MICROPOLAR ELASTOPLASTICITY

Ákos Gombos and László Szabó

Department of Applied Mechanics
Budapest University of Technology and Economics
Műegyetem rkp. 5., H-1111 Budapest, Hungary
E-mail: gombos@mm.bme.hu, szabo@mm.bme.hu

Keywords: micropolar elastoplasticity, stress updating, consistent tangent operator.

Summary. *This paper is concerned with the computational analysis of elastoplastic micropolar solids at small deformation. A stress updating integration algorithm is derived and an explicit expression is deduced for the consistent tangent operator. The applicability and the performance of the proposed numerical method are illustrated by sevaral three dimensional finite element applications.*

1 INTRODUCTION

The micropolar continuum model have been fairly extensively analysed in the last decad. The micropolar theory have been employed to the J_2-flow theory by de Borst [2], Willam at el. [6], and to the deformation theory by Mülhaus and Vardoulakis [5] in two dimensional range at small deformation. A more general elastoplastic micropolar models in the large deformation range developed by Forest [3] and Grammenoudis and Tsakmakis [4]. However, despite considerable theoretical and computational contributions made in the computational analysis of micropolar continua, many questions are still unanswered and useful formulations similar to the classical continuum plasticity are not available in the literature.

The purpose of this paper is to develop a stress updating algorithm to elastoplastic micropolar solid, and to derive the corresponding consistent (algorithmic) tangent operator to three dimensional case at small deformation. The elastic part of the constitutive model is based on the Eringen's [1] micropolar theory, and the plastic part is defined by an extended flow theory of plasticity.

2 CONSTITUTIVE RELATIONS FOR MICROPOLAR SOLIDS

The kinematic equations for micropolar continuum at small deformation are of the form [1]:

$$\boldsymbol{\varepsilon} = \mathrm{grad}^T \mathbf{u} + (\boldsymbol{\epsilon} \cdot \boldsymbol{\phi})^T, \qquad \boldsymbol{\gamma} = \mathrm{grad}\boldsymbol{\phi}, \tag{1}$$

where $\mathbf{u}$ is the displacement vector, $\boldsymbol{\phi}$ is the microrotation vector, $\boldsymbol{\varepsilon}$ and $\boldsymbol{\gamma}$ are the strain measures.

The rate form of the elastic-plastic constitutive equations in the case of small deformation can be summarized as

$$\dot{\mathbf{t}} = \mathbf{A}^e : (\dot{\boldsymbol{\varepsilon}} - \dot{\boldsymbol{\varepsilon}}^p), \qquad \dot{\mathbf{m}}^T = \mathbf{B}^e : (\dot{\boldsymbol{\gamma}} - \dot{\boldsymbol{\gamma}}^p), \quad \dot{\boldsymbol{\varepsilon}}^p = \lambda \frac{\partial F}{\partial \mathbf{t}}, \quad \dot{\boldsymbol{\gamma}}^p = \lambda \frac{\partial F}{\partial \mathbf{m}^T}, \quad \dot{\alpha} = \lambda h(\mathbf{t}, \mathbf{m}), \tag{2}$$

where $\mathbf{t}$ is the stress, $\mathbf{m}$ is the couple stress tensor, and $\mathbf{A}^e$ and $\mathbf{B}^e$ are the fourth-order elastic constitutive moduli, λ is the plastic multiplier, α is the hardening parameter.

The extended form of the von Mises yield condition is defined by

$$F(\mathbf{t}, \mathbf{m}, \kappa(\alpha)) = f(\mathbf{t}, \mathbf{m}) - \frac{1}{3}\kappa^2(\alpha) \equiv \frac{1}{2}\left(\mathbf{t} : \mathbf{T} : \mathbf{t} + \mathbf{m}^T : \mathbf{M} : \mathbf{m}^T\right) - \frac{1}{3}\kappa^2(\alpha) \leq 0, \tag{3}$$

where the fourth-order tensors $\mathbf{T}$ and $\mathbf{M}$ defined as $(\mathbf{T})_{ijkl} = \frac{1}{2}(1 + a_1)\delta_{ac}\delta_{bd} + \frac{1}{2}(1 - a_1)\delta_{ad}\delta_{bc} - \frac{1}{3}\delta_{ab}\delta_{cd}$, $(\mathbf{M})_{ijkl} = \frac{1}{2}(b_1 + b_2)\delta_{ac}\delta_{bd} + \frac{1}{2}(b_1 - b_2)\delta_{ad}\delta_{bc} - \frac{1}{3}\delta_{ab}\delta_{cd}$, here $a_1, b_1$and b_2 are the micropolar material parameters. The yield function defined above is obtained by a consistent derivation of distortion strain energy, so it represents by the deviatoric part of $\mathbf{t}$ and $\mathbf{m}$.

3 STRESS UPDATING AND CONSISTENT TANGENT OPERATOR

In this work, the implicit backward Euler method is employed to determine the updated stress and plastic state variables. In the strain driven problem, the Newton-Raphson iteration privides the strain $\boldsymbol{\varepsilon}_{n+1}$ and torsion $\boldsymbol{\gamma}_{n+1}$ values which use to define the stress and couple stress at step $n+1$ as

$$\mathbf{t}_{n+1}=\mathbf{t}_{n+1}^{trial}-\Delta\lambda\mathbf{A}^{e}:\left.\frac{\partial f}{\partial\mathbf{t}}\right|_{n+1}\qquad\mathbf{m}_{n+1}^{T}=\left(\mathbf{m}_{n+1}^{trial}\right)^{T}-\Delta\lambda\mathbf{B}^{e}:\left.\frac{\partial f}{\partial\mathbf{m}^{T}}\right|_{n+1}, \tag{4}$$

where $\mathbf{t}_{n+1}^{trial}$ and $\mathbf{m}_{n+1}^{trial}$ are the so-called trial stress and couple stress, respectively. The set of equations (4) with the yield condition $F_{n+1}(\mathbf{t}_{n+1},\mathbf{m}_{n+1},\kappa\left(\alpha_{n+1}\right))=0$ a set of nonlinear equation in terms of values $\mathbf{t}_{n+1}$, $\mathbf{m}_{n+1}$ and $\Delta\lambda$ which is effectively solved by a local Newton iterative procedures. It is important to note that in the case of perfect plasticity or linear isotropic hardening a closed form exact solution is possible.

The consistent tangent operator is essential to preserve the quadratic rate of asymptotic convergence of global Newton-Raphson iteration. To derive this quantity, equation (4) is differentiated to give

$$d\mathbf{t}_{n+1} = \mathbf{D}_{\varepsilon}:d\Delta\boldsymbol{\varepsilon}-d\Delta\lambda\mathbf{N}_{t},\quad\mathbf{D}_{\varepsilon}=\left(\mathbf{A}^{e-1}+\Delta\lambda\frac{\partial^{2}f}{\partial\mathbf{t}\partial\mathbf{t}}\right)^{-1},\quad\mathbf{N}_{t}=\mathbf{D}_{\varepsilon}:\frac{\partial f}{\partial\mathbf{t}} \tag{5}$$

$$d\mathbf{m}_{n+1}^{T} = \mathbf{D}_{\gamma}:d\Delta\boldsymbol{\gamma}-d\Delta\lambda\mathbf{N}_{m},\quad\mathbf{D}_{\gamma}=\left(\mathbf{B}^{e-1}+\Delta\lambda\frac{\partial^{2}f}{\partial\mathbf{m}^{T}\partial\mathbf{m}^{T}}\right)^{-1},\quad\mathbf{N}_{m}=\mathbf{D}_{\gamma}:\frac{\partial f}{\partial\mathbf{m}^{T}}. \tag{6}$$

Using the consistency condition $dF\left(d\Delta\lambda\right)=0$, the plastic multiplier can be expressed as $d\Delta\lambda=\frac{1}{h}\left(\mathbf{N}_{t}:d\Delta\boldsymbol{\varepsilon}+\mathbf{N}_{m}:d\Delta\boldsymbol{\gamma}\right)$, where $h=\frac{\partial f}{\partial\mathbf{t}}:\mathbf{N}_{t}+\frac{\partial f}{\partial\mathbf{m}^{T}}:\mathbf{N}_{m}+\frac{2}{3}\kappa\left(\alpha_{n+1}\right)\frac{\partial\kappa\left(\alpha_{n+1}\right)}{\partial\Delta\alpha}h\left(\mathbf{t}_{n+1},\mathbf{m}_{n+1}\right)$.

By combining these equations defined above, the consistent tangent relations takes the following form

$$\left[\begin{array}{c}d\mathbf{t}\\ d\mathbf{m}^{T}\end{array}\right]=\left[\begin{array}{cc}\mathbf{D}_{\varepsilon}-\frac{1}{h}\mathbf{N}_{t}\otimes\mathbf{N}_{t} & -\frac{1}{h}\mathbf{N}_{t}\otimes\mathbf{N}_{m}\\ -\frac{1}{h}\mathbf{N}_{m}\otimes\mathbf{N}_{t} & \mathbf{D}_{\gamma}-\frac{1}{h}\mathbf{N}_{m}\otimes\mathbf{N}_{m}\end{array}\right]\left[\begin{array}{c}d\Delta\boldsymbol{\varepsilon}\\ d\Delta\boldsymbol{\gamma}\end{array}\right]. \tag{7}$$

It should be note that the inversion in tensors $\mathbf{D}_{\varepsilon}$ and $\mathbf{D}_{\gamma}$ can be evaluated in a closed form.

The method is intended for use in finite element calculations that employ the micropolar plasticity model in small deformation range. The algorithm and the consistent tangent operator has been implemented in a finite element code based on 20-noded solid element type. Some full three dimensional numerical examples are presented that demonstrate the capability and accuracy of the proposed algorithm.

ACKNOWLEDGMENT

This research has been supported by the National Development and Research Foundation, Hungary (under Contract: OTKA, T046488). This support is gratefully acknowledged.

REFERENCES

[1] Eringen, A.C. (1999): *Microcontinuum Field Theories,* Springer Verlag, Berlin.

[2] De Borst, R. (1993): A generalisation of J_2-flow theory for polar continua. *Comp. Meth. Appl. Mech. Engng*, Vol. 103**,** pp. 347-362.

[3] Forest, S., Sievert R. (2003): Elastoviscoplasticity constitutive frameworks for generalized continua. *Acta Mechanica,* Vol. 160, pp. 71-111.

[4] Grammenoudis, P., Tsakmakis, Ch. (2005): Finite element implentation of large deformation micropolar plasticity exhibiting isotropic and kinematic hardening effect. *Int. J. Num. Meth. Engng.*, Vol. 62**,** pp. 1691-1720.

[5] Mülhaus, H.-B., Vardoulakis, I. (1987): The thickness of shear bands in granular materials. *Géotechnique,* Vol. 37**,** pp. 271-283.

[6] Willam, K., Dietsche, A., Iordache, M-M., Steinmann, P. (1995): *Localization in Micropolar Continua*, In: Mühlhaus, H.-B. (Ed.), Continuum Models for Materials with Microstructure. John Wiley & Sons, Chichester, pp. 1-25.

6th European Solid Mechanics Conference
ESMC 2006
28 August – 1 September, 2006
Budapest, Hungary

NUMERICAL ANALYSIS OF PERIDYNAMIC MATERIAL MODEL WITH RADIAL BASIS FUNCTION METHOD

Gábor Ladányi[1]

[1]Department of Applied Mechanics
Budapest University of Technology and Economics
P.O. Box 91, 1521 Budapest, Hungary
E-mail: ladanyi@mail.duf.hu

Keywords: peridynamic nonlocal material, RBF, meshless

Summary. *One of the greatest drawback of the classical elasticity is the lack of discontinuities. The peridynamic material model of Silling et al. can solve this problem and in other hand using this there is no need of any additional technique to enforce the natural boundary conditions in meshless methods. In this paper a simple example shows this second feature of peridynamic material model.*

1 INTRODUCTION

The meshless methods are known as good alternatives to eliminate the disadvantages of finite element method. For example using them the handling of discontinues are possible. One of the simplest meshless method is the Radial Basis Functions method (RBF), but like others, it suffers from the difficulties of enforcement of boundary conditions because meshless shape functions suffice the Kronecker condition on the nodal points. To eliminate this problem in the last decade many solutions were born, like Lagrange-multipliers, penalty methods [1].
In the classical theory of elasticity the main variable is the displacement. Usually, the numerical determination of this is made with approximation of the equilibrium equations, but in them only the derivatives of displacement appear.
In 2000, Silling S. A. has introduced a new material model, the peridynamic type. Using it the problem of natural boundary conditions and discontinous displacement field can be solved in one hand.

2 DEFINITION OF PERIDYNAMIC MATERIAL

Let Ω be the set on the inner points of a solid body, Γ_u the boundary with prescribed movement and Γ_t the boundary with surface load.
Let $X, Y \in \Omega$ two points of the body, $\mathbf{u}$ the displacement and $\mathbf{b}$ the body load at the point X. By the

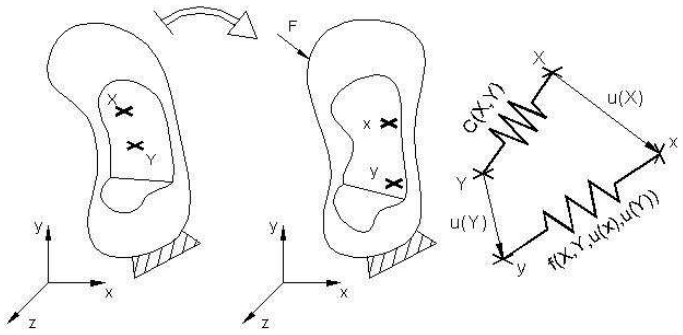

Figure 1: Peridynamic inner force between two points

hypothesis of peridynamic material model, during the motion, there is an $\mathbf{f}(X, Y, u(X), u(Y))$ pairwise force between X and Y (see Figure 1). As in the work of Silling and co. [2] can be found, with the

introduction of $\xi = Y - X$ and $\eta = u(Y) - u(X)$ variables the pairwise force function must have next features:

$$\mathbf{f}(-\eta, -\xi) = -\mathbf{f}(\eta, \xi); \mathbf{f}(\eta, \xi) = \mathbf{F}(\eta, \xi) \cdot (\eta + \xi). \tag{1}$$

In case of small displacements and linear microelastic material, the function $\mathbf{f}$ is linear function of η and it can be written in $\mathbf{f}(\eta, \xi) = \mathbf{C}(\xi) \cdot \eta$ form. Assuming these properties the equilibrium equation of an inner point has new shape:

$$\int_{\Omega \bigcup \Gamma_t} \mathbf{C}(\xi) \cdot (u(Y) - u(X)) dY - \int_{\Gamma_u} \mathbf{C}(\xi) \cdot u(X) dY = -\int_{\Gamma_u} \mathbf{C}(\xi) \cdot \hat{\mathbf{u}}(Y) dY - \mathbf{b}(X). \tag{2}$$

The (2) equation is a Fredholm-type integral equation of the second kind. The numerical solution of these equations is possible on quite wide range of function spaces by many techniques, like collocation, least-square or Galerkin method.

3 RADIAL BASIS SIMULATION IN THE CASE OF HOOKEAN PLANE STRESS PROBLEMS

In present work an uniconstant Hookean material was modelled. An inner nonlocal spring was assumed between every two point of the body with semi-Hookean behavior. The distribution theory was used to describe this phenomena with Gaussian distribution function where l_r was the characteristic length of material. Introducing the $\lambda = \xi/|\xi|$ vector the kernel function of (2) was

$$\mathbf{C}(X, Y) = E\delta''(|Y - X|) \cdot \lambda \otimes \lambda \rightarrow \mathbf{C}(X, Y) = E \cdot \frac{\partial^2}{\partial \xi^2}\left(\frac{e^{\xi^2/l_r^2}}{\pi \cdot l_r^2}\right) \cdot \lambda \otimes \lambda. \tag{3}$$

Let X_j and X_k nodal points in Ω and Γ_u, respectively. If $[N]$ is the matrix of radial basis functions [3] and $\{U\}$ is the vector of nodal coefficients, then from (2) integral equation and the natural boundary conditions, an asymmetric system of collocation equations can be set.

$$\left[\int_{\Omega \cup \Gamma_t} \mathbf{C}(\xi) \cdot (N(Y) - N(X_j)) dY - \int_{\Gamma_u} \mathbf{C}(\xi) \cdot N(X_j) dY\right]\{U\} = \{-\int_{\Gamma_u} \mathbf{C}(\xi) \cdot \hat{\mathbf{u}}(Y) dY - \mathbf{b}(X_j)\} \tag{4}$$

$$[N(X_k)]\{U\} = \{\hat{\mathbf{u}}(X)\}. \tag{5}$$

The presented example is a $1mm$ wide plate with $b = 1N/mm^3$ uniaxial volumetric load. (Figure 2) shows the convergence of numerical solution to the analytical solution (u_a) with 175, 324 and 637 nodal points.

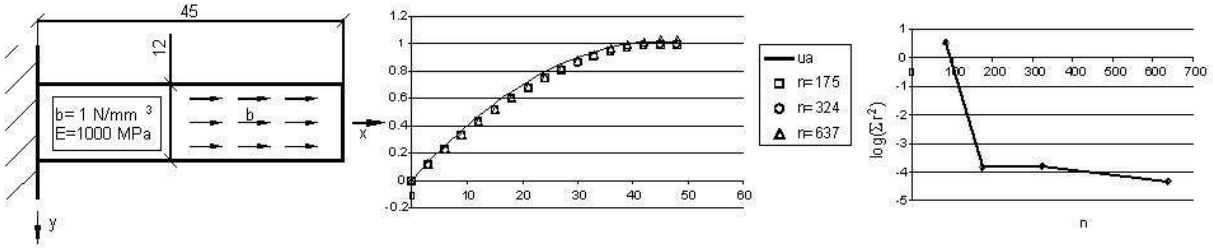

Figure 2: Plate with uniaxial load: solution and convergence

REFERENCES

[1] Atluri, S. N., Shen, S. (2001): *The Meshless Local Petrov-Galerkin (MLPG) Method*, Tech Science Press, Forsyth.

[2] Silling, S. A. (2000): Reformulation of Elasticity Theory for Discontinuities and Long-Range Forces, *J. Mech. Phys. Solids*, Vol. 48, pp. 175-209.

[3] Larson, E., Fornberg B. (2003): A Numerical Study of Some Radial Basis Function Based Solution Methods for Elliptic PDEs, *Computers and Mathematics with Applications*, Vol. 46, pp. 891-902.

Numerical analysis of peridynamic material with moving least square method

Gábor Ladányi[1]

Abstract: *The meshless methods are known as robust and well-known solutions of problems in elasticity, especially on the field of crack mechanics. On of the greatest difficulty of meshless methods is the enforcement of boundary conditions. In our text we introduce a new type of nonlocal material, the peridynamic material, that can solve these problems. After some theoretical words we show sample problems to demonstrate the abilities of this material.*

Keywords: peridynamic material, nonlocal elasticity, MLS.

1 Introduction

The meshless methods are known as good alternatives to eliminate the disadvantages of finite element method. For example, by using them the handling of discontinuities is possible. One of the simplest methods is the moving least square method (MLS), but like others, it suffers from the problem of enforcement of boundary conditions. These difficulties originate from a special feature of meshless shape functions. They do not suffice the Kronecker condition on nodal points. In the last decade many solutions were born to eliminate this problem, eg. Lagrange-multipliers, penalty methods, still this field is one of the most researched of all recently.
In the classical theory of elasticity the main variable is the displacement. Usually the numerical determination of it is made with approximation of equilibrium equations, but only the derivatives of displacement appear in them.
In 1998, Silling S. A. introduced a new material model, the peridynamic type. Using of it equilibrium equations contain dirrectly the displacements, so the natural boundary conditions can be applied immediately.

2 Definition of peridynamic material

Let Ω be the set on the inner points of a solid body and Γ be the boundary of Ω. We are going to use the closure of Ω, the $\overline{\Omega} := \Omega \overset{S}{} \Gamma$. In the classical problem of elasticity the boundary of the body can be split to two regions, the Γ_u, where the movements of the points are known and Γ_t, where the surface load is given. We strictly require the $\Gamma_u \cup \Gamma_t = \Gamma$ and $\Gamma_u \cap \Gamma_t = \oslash$ features. Let $X \in \overline{\Omega}$ be the coordinate of a point in the unload state, and be $\mathbf{u}(X) : \mathrm{R}^3 \mapsto \mathrm{R}^3$ the movement of X. Let $A_u(X) : \mathrm{R}^3 \mapsto \mathrm{R}^3$ be an operator that order the sum of the inner forces to X. Then the above boundary conditions can be written as:

$$\{\mathbf{u}(X) \equiv \hat{u}(X); X \in \Gamma_u\} \tag{1}$$

[1]Phd. student of Budapest University of Technology and Economics, Budapest (ladanyi@mail.duf.hu).

$$\{A_u(X) \equiv \hat{\mathbf{t}}(X); X \in \Gamma_t\} \tag{2}$$

The hypothesis of peridynamic material says that, during the motion of body there is an $\mathbf{f}(X, Y, \mathbf{u}(X), \mathbf{u}(Y))$ pairwise force between the X and Y points. With the introduction of $\eta = Y - X$ and $\xi = \mathbf{u}(Y) - \mathbf{u}(X)$ variables $\mathbf{f}$ will be simpler $\mathbf{f} = \mathbf{f}(\eta, \xi)$. The pairwise force function must have the next features[6]:

$$\mathbf{f}(-\eta, -\xi) = -\mathbf{f}(\eta, \xi) \tag{3}$$

$$\mathbf{f}(\eta, \xi) = F(\eta, \xi) \cdot (\eta + \xi) \tag{4}$$

In the case of small displacements and linear microelastic material $\mathbf{f}$ is linear function of ξ:

$$\mathbf{f}(\eta, \xi) = \mathbf{K}(\xi) \cdot \eta \tag{5}$$

3 Analysis of equilibrium equation

Let $\mathbf{q}(X)$ be the volumetric force in Ω, then the equation of equilibrium is:

$$\int_{\overline{\Omega}} \mathbf{f}(X, Y, \mathbf{u}(X), \mathbf{u}(Y)) dY + \mathbf{q}(X) = \mathbf{0}; X \in \Omega \tag{6}$$

The shape of equation is the function of the position X and, the (6) is valid only in the Ω, but should be completed on Γ_t boundary. Introducing the general load function

$$\{\mathbf{s}(X) = \delta_\Omega(X) \cdot \mathbf{q}(X) + (1 - \delta_\Omega(X)) \cdot \hat{\mathbf{t}}(X); X \in \overline{\Omega}\} \tag{7}$$

with δ_Ω inner Dirac-delta function, a new equation can be written:

$$\{\int_{\overline{\Omega}} \mathbf{f}(X, Y, \mathbf{u}(X), \mathbf{u}(Y)) dY + \mathbf{s}(X) = \mathbf{0}; X \in \overline{\Omega}\} \tag{8}$$

which is valid on all the $\overline{\Omega}$. In the next session we see only the case of linear elastic material. The (8) equation, splitting the support of integral, is:

$$\{\int_{\Omega \cup \Gamma_t} \mathbf{K}(X, Y) \cdot (\mathbf{u}(Y) - \mathbf{u}(X)) dY - \int_{\Gamma_u} \mathbf{K}(X, Y) \cdot \mathbf{u}(X) dY = \mathbf{p}(x); X \in \overline{\Omega}\} \tag{9}$$

where:

$$\mathbf{p}(X) := -\int_{\Gamma_u} \mathbf{K}(X, Y) \cdot \hat{\mathbf{u}}(Y) dY - \mathbf{s}(X) \tag{10}$$

The (9) equation is a Fredholm-type integral equation of the second kind. The numerical solution of these equations is possible on a quite wide range of function spaces by many technics, like collocation, least-square or Galerkin method.

4 Numerical approximation in the case of plane stress problems

In plane stress problems the displacement function is

$$\mathbf{u}^T(X) = [\ u(X) \quad v(X)\ ] \tag{11}$$

Let $\{X_I^{(Node)} \in \overline{\Omega}; I = [1..NP]\}$ be the set of nodal points with associated $\mathbf{N}(X)$ vector of shape functions. Then $\tilde{\mathbf{u}}(X)$, the approximate displacement function is

$$\tilde{\mathbf{u}}(X) = \mathbf{N}(X) \cdot \mathbf{U} \tag{12}$$

where $\mathbf{U}$ is the vector of nodal coefficients.
In our numerical tests we used the Galerkin method to determine the values of the $\mathbf{U}$ variables. Let us introduce the pointwise residues and the volumetric integral of its square:

$$\mathbf{r}(X) := \int_{\Omega \cup \Gamma_t} \mathbf{K}(X,Y) \cdot (\tilde{\mathbf{u}}(Y) - \tilde{\mathbf{u}}(X)) dY - \int_{\Gamma_u} \mathbf{K}(X,Y) \cdot \hat{\mathbf{u}}(X) dY - \mathbf{p}(X) \tag{13}$$

$$R = \int_{\overline{\Omega}} \mathbf{r}^2(X) dX \tag{14}$$

With the minimization of R by $\mathbf{U}$ variables the determination of approximation is possible and it is equal with the Galerkin solution. This minimization leads to a set of linear equations:

$$\mathbf{M} \cdot \mathbf{U} = \mathbf{f} \tag{15}$$

where

$$\mathbf{M} = \int_{\overline{\Omega}} (\mathbf{N}^T(X) \cdot (\int_{\Omega \cup \Gamma_t} \mathbf{K}(X,Y) \cdot (\mathbf{N}(Y) - \mathbf{N}(X)) dY - \int_{\Gamma_u} \mathbf{K}(X,Y) \cdot \mathbf{N}(X) dY) dX \tag{16}$$

$$\mathbf{f} = \int_{\overline{\Omega}} (\mathbf{N}^T(X) \cdot (- \int_{\Gamma_u} \mathbf{K}(X,Y) \cdot \hat{\mathbf{u}}(Y) dY - \mathbf{s}(X))) dX \tag{17}$$

The $\mathbf{N}(X)$ shape functions can be chosen from many function spaces. In our examples we used the moving least square method, when shape functions are determined by the minimization of weighted error-square [2]. With using polynomial basis the moving least square shape function can be written as:

$$\tilde{\mathbf{u}}(X) = \mathbf{p}^T(X) \cdot \mathbf{a}(X) \tag{18}$$

where

$$\mathbf{a}(X) = \mathbf{A}^{-1}(X) \cdot \mathbf{C}(X) \cdot \mathbf{U} \tag{19}$$

$$\mathbf{A}(X) = \sum_{I=1}^{NP} w(X - X_I) \cdot \mathbf{p}(X_I) \cdot \mathbf{p}^T(X_I) \tag{20}$$

$$\mathbf{C}(X) = [w(X - X_1) \cdot \mathbf{p}^T(X_1, w(X - X_2) \cdot \mathbf{p}^T(X_2, .., w(X - X_{NP}) \cdot \mathbf{p}^T(X_{NP}] \tag{21}$$

With the equations (19), (20) and (21) the shape function can be written as:

$$\mathbf{N}(X) = \sum_{j=1}^{m} p_j(X)(\mathbf{A}^{-1}(X) \cdot \mathbf{C}(X)) \tag{22}$$

One of the first problems that appeared in scientific papers were the difficult handling of natural boundary conditions in meshfree methods [4]. Since the early times more technics were published to solve this, like penalty [7], Lagrange-multiplier[1], inverse matrix and coupling with finite elements method. In spite of this nowadays it is an active field of research. As we mentioned, the equilibrium equations of peridynamic material contain the natural boundary conditions, so there is no need of any addition technic to enforce boundary conditions, they appear in the force vector and the solution will be good on the boundary in the term of least square.
We have to note that with pure application of this theory the constraints of the body are going to be linear elastic springs with the same elastic moduli like the body's material.

5 Calibration and applications

In the term of (9) the pairwise force between X and Y points is determined by the K kernel function of the integral equation. From statical viewpoint K must be symmetric in X and Y so it can be the function only $|\xi|$. In our samples we used the

$$\mathbf{K}(\xi,\eta) = \lambda(|\xi|)\cdot\xi\otimes\xi \tag{23}$$

form, which satisfies the requirements. We have quite freedom in the choosing of λ, and we used the simplest possibility:

$$\lambda(|\xi|) = \begin{cases} c\cdot E, & |\xi| \le r_{mat}; \\ 0, & |\xi| > r_{mat}. \end{cases}$$

This function is finite supported which is suggested by nonlocal real materials, where r_{mat} is the

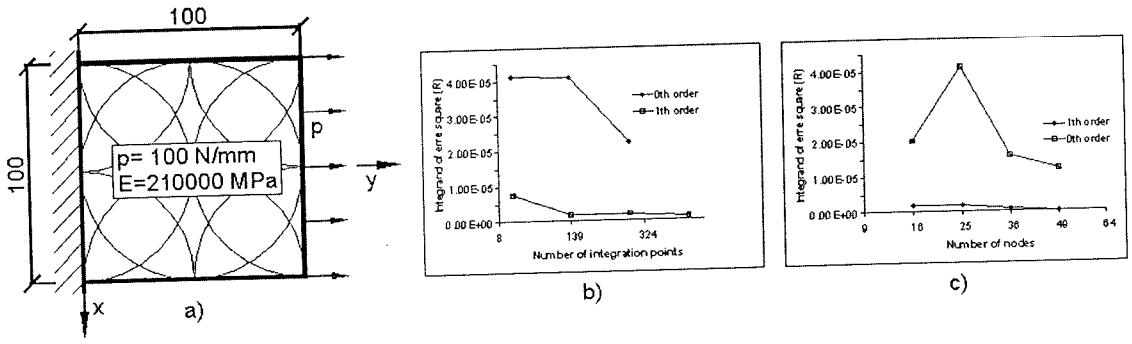

Figure 1: Uniaxial loaded plate: a)configuration b)convergence in integral points c)convergence in nodal points

radius of maximum range of internal forces. For the determination of c we made a numerical experiment serie on an uniaxial loaded plate with $r_{mat} = 0.1mm$ (fig.1). The analitical solution of this problem predicts the longitudinal strain as:

$$\Delta L = N\cdot L/(A\cdot E) = 0.05mm \tag{24}$$

From successive approximation we found the material c must be:

$$c(\xi) = \pi/\xi^2 \tag{25}$$

As the error estimator we used the R from (14) and examined the convergence of integration and numerical solution. The nodals and the integration points were put regularly into the body. We used Gauss integration to calculate the outer and inner integrals, too. The second example was plate with pure share and examined the movements of the body and convergence of the solution. This model inherited the geometry and material constants from the previous example. The configuration can be seen on (fig.2). The analytical solution of a linear elastic plate predicts the linear motion in x and in y direction. In our example we tested the difference from this linearity in x dirrection. The analytical predicted displacement was

$$u_a(X) = u(0) + (u(L) - u(0))/L\cdot X \tag{26}$$

The integral of square of difference between $u_a(X)$ and $\tilde{u}(X)$ characterize the error of approximation(fig.2).

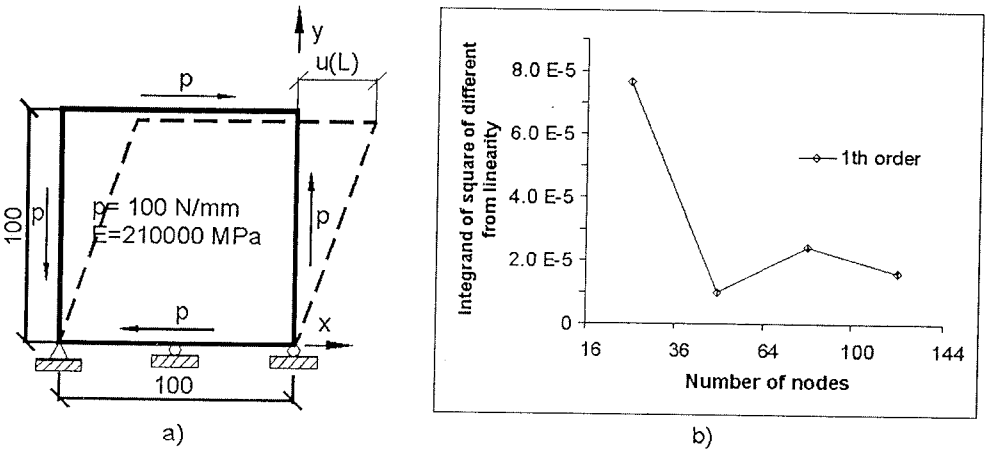

Figure 2: Plate with pure shear: a)configuration b)integral of square of different from linearity

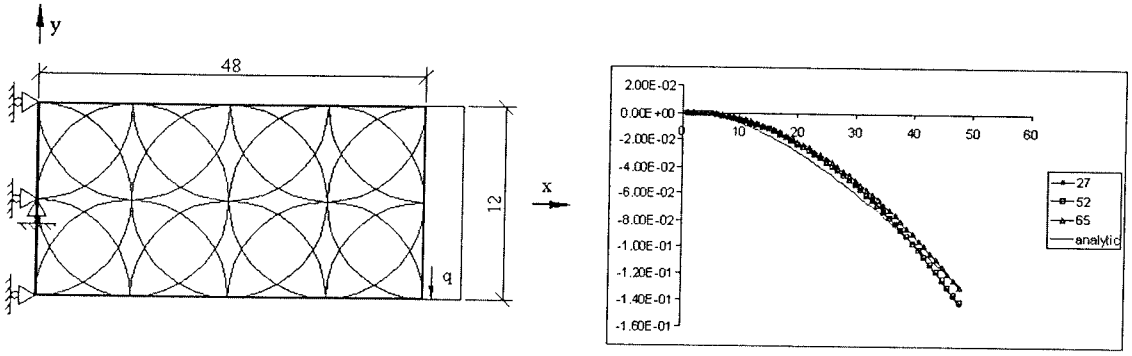

Figure 3: The v(x)displacement of a cantilever beam, with 3x9, 4x13 and 5x13 nodes

The last example was a cantilever beam with uniform load at the end. The (fig.3) shows the geometry and configuration of the cantilever beam. In this example we tested the character of the movement in y dirrection. From the beam theory it must be:

$$v_a(X,0) = F/(IE) \cdot (Lx^2/2 - x^3/6) \tag{27}$$

6 Conclusion

We have presented a study of a new nonlocal elastic, the peridynamic, material. We introduced and derived the numerical approximation of the simplest linear elastic material. We emphasized the benefits of peridynamic material versus Hookean material on the enforcing of natural boundary conditions.

In our first example we showed the way how a peridynamic model can be calibrated to approximate a Hookean model. The second and the third examples transparented the boundary conditions and the convergence of solutions.

References

[1] Belytschko T., Krongauz Y., Organ D., Fleming M., Krysl P.,"Meshless Methods: an Overview and Recent Developments", in International Journal for Numerical Methods in Enginnering, 139., pp:3-47, Elsevier., 1996.

[2] Belytschko T., Organ D., Gerlach C.,"Element-free Galerkin methods for dynamic fracture in concrete", in Computer Methods in Applied Mechanical Engineering, 187., pp:385-399, Elsevier., 2000.

[3] Cueto E., Garcia L., Doblareand M., "Impossing essential boundary conditions in the Natural Element Method by means of density-scaled alpha-shapes", in International Journal for Numerical Methods in Engineering 49, pp:519-546, Elsevier., 2000.

[4] Günther F. C., Liu W. K.,"Implementation of Boundary Conditions for Meshless Methods", in Computer Methods in Applied Mechanics and Engineering, pp:111-121, Elsevier., 1997.

[5] Rao B. N., Rahman S.,"A coupled meshless-finite element method for fracture analysis of cracks", in International Journal of Pressure Vessels ans Piping 78, pp:647-657, Elsevier., 2001.

[6] Silling S. A., "Reformulation of Elasticity Theory for Discontinuities and Long-Range Forces", SAND98-2176 Unlimited Release Printed, Sandia National Laboratories, 1998 .

[7] Zhu T., Atluri S. N.,"A modified collocation method and a penalty formulation for enforcing the essential boundary conditions in the element free Galerkin method", in Computational Mechanics , 21., pp:211-222, Springer-Verlag., 1998.